

Behaviour of rubberized cement-bound aggregate mixtures containing different stabilization levels under static and cyclic flexural loading

Ahmed Hilal Farhan^{1,*}, Andrew Dawson², Nick Thom²

¹ Civil Engineering Department, University of Anbar, Main Campus, Anbar, Iraq.

Tel: +964 7805521276, E-mail: ahmed.farhan2010@yahoo.com, ahmed.farhan_ce@uoanbar.edu.iq

² School of Civil Engineering, Faculty of Engineering, University of Nottingham, University Park, Nottingham NG7 2RD, UK

*corresponding author

Abstract

An investigation has been undertaken to investigate the influence of rubber inclusion at different levels of stabilization on the behaviour of cemented granular mixtures, under static and cyclic flexural testing, and to compare this with mixtures without rubber. Both are intended to be used as base courses of semi-rigid pavement structure. 3%, 5%, and 7% of cement by dry weight of aggregate were used for stabilization purposes. Rubberization of cemented aggregate was conducted by replacing 30% of the aggregate of the 6 mm fraction size by an equivalent rubber volume. The investigated properties were flexural strength, static and dynamic stiffness moduli, toughness and fatigue life. Damage due to cyclic loading was evaluated in terms of stiffness degradation and permanent deformation accumulation. Flexural-induced cracking behaviour was also investigated. Results reveal that the rate of flexural strength increase is higher for the reference cemented mixtures. As stabilizer quantity increase, both static and dynamic stiffness moduli increased while rubberization mitigated these two parameters at all stabilizer contents. Toughness and fatigue life were improved due to rubber modification at investigated stabilizer contents. Flexural-induced cracks always tend to propagate through rubber aggregate regardless of the quantity of cement.

Keywords: Rubberized cement-stabilized aggregate; flexural testing; fatigue life; modulus of elasticity, cracking pattern.

1 Background

In the light of the consequences of current climate change and due to the expansion of the world, solid waste management and saving of natural resources have become high priorities. One of the most important waste materials is post-consumer tires since the number of disposed tires has increased dramatically year on year. In western and eastern European countries, Middle East, Japan, Latin America, North America, about 500 million old tires are discarded every year as statistics reveal (Oikonomou and Mavridou 2009). Stockpiling and combustion, to provide fuel, are the main usage of discarded tires at present time. Both of these are, unfortunately, not environmentally sound solutions. However, extensive research into using tire-derived rubber in concrete mixtures, conducted over the last thirty years by many scholars (Topcu and Avcular 1997, Güneyisi et al. 2004, Khaloo et al. 2008, Pelisser et al. 2011, Eiras et al. 2014, Youssf et al. 2016), has confirmed that rubber derived from old vehicle tires when they incorporated in concrete mixtures affects both strength and stiffness detrimentally. This represents an obstacle limiting their use in structural applications. To mitigate these disadvantages and to improve the properties of rubberized concrete mixtures, an effort was conducted to enhance the adhesion between rubber aggregate and adjacent materials. Güneyisi et al. (2004), Pelisser et al. (2011) and Youssf et al. (2016) attributed the poor properties of rubberized mixture to the less adhesive nature of rubber aggregate particles. Therefore, some attempts were conducted to achieve such adhesion improvement. These are using sodium hydroxide to ensure proper roughness of rubber and also improving the interaction between rubber and other components by using silica fume. The findings indicated some improvement in performance.

As pavement structures consumes large quantity of natural materials, replacing the latter materials with rubber aggregate will ensure a higher degree of sustainability compared with other applications (Cao 2007, Barišić et al. 2014). This may be the reason that many studies conducted recently have used different recycled and waste materials such as recycled concrete aggregate (Li et al. 2010), recycled asphalt pavement RAP (Puppala et al. 2017), glass materials (Arulrajah et al. 2015) and construction and demolition waste CDW (Xuan et al. 2012) for potential use in highway construction. However, very few studies have investigated the use of rubber in cement-stabilized aggregate mixtures with relatively low cement contents to be used in the pavement base course layer. Recently, Farhan et al. (2015) studied the influence of different amount of tire rubber aggregate on the flexural behaviour of cement-bound aggregate mixtures, and Farhan et al. (2016) studied the behaviour of rubberized cemented mixtures with different cementation levels under indirect tensile loading. However, few researches have reported the effect of cement content on the flexural behaviour of cement-stabilized mixture with and without rubber aggregate particles. Moreover, these stabilized mixtures when used in a pavement structure are normally subjected to vehicular cyclic loading. This necessitates, for better understanding, measurement of their behaviour under such loading conditions.

2 Significance and objectives

One of the most important steps necessary to allow the beneficial use of waste tires within cement-bound pavement layers is to understand how the inclusion of these waste materials at different cement contents may influence the final behaviour when subjected to flexural loading. Flexural testing was selected due to its close simulation of field conditions. As pavement structures are subjected to cyclic loading due to the movement of vehicles, the behaviour was also evaluated under cyclic loading.

Cracking in cement-bound mixtures usually develops due to tensile stresses. As cracking represents the main disadvantage of using cemented layers due to reflection of these cracks through the overlying layers, studying the role that cement content plays on cracking tendency and pattern is the key to optimizing mix design. Limited information has been found regarding quantitative investigation of cracking patterns of cement-bound mixtures.

The objectives of this study are, firstly, to show the effect of cement quantity, mainly on the static and cyclic flexural behaviour and to characterize quantitatively the cracking behaviour of both conventional and rubberized cement-bound aggregate mixtures (CBAMs and RCBAMs).

3 Materials and preparation

3.1 Materials and their characterization

Limestone aggregate (20 mm maximum size) was used in this study. This type of aggregate consists of different nominal size fractions. Rubber from recycled tires was used in this investigation. The gradation of both rubber and different aggregate size fraction are as stated in (Farhan et al. 2016b). Portland cement was used for stabilization of aggregate mixture. For the purpose of compaction and hydration of cement, water from the public supply was used. Table 1 shows the properties of cement used in this study while Table 2 presents the properties of aggregate.

3.2 Mix Design

Since there are many types of Cement-Bound Granular Mixtures (CBGM) with maximum aggregate sizes of 10, 14, 20 and 45 mm, the moderate aggregate maximum size value was selected for the purpose of this study. To achieve the gradation of the (CBGM2-0/20) as specified in (BS EN 14227-1:2013), the combination of different aggregate fractions was achieved on the basis of weight proportions using trial and error method (Garber and Hoel 2009). These proportions were as follows: 11% of 20mm, 20% of 14mm, 11% of 10mm, 13% of 6 mm

and 45% of particles less than 6mm. The design aggregate mixture gradation is shown in Figure 1. The stabilization of mixtures was conducted using cement content of 3%, 5% and 7% by dry weight of aggregate. These were selected based on the range studied by (Thompson 2001). Due to its size similarity with that of rubber particles, the 6 mm size was selected for partial replacement by rubber to ensure the same aggregate packing. Therefore, rubberized mixtures were constituted by replacing 30% of the volume of this fraction by an equivalent volume of tire-derived rubber aggregate which equals about 3.9% by the volume of the total aggregate mixture. The design water quantity for each cement content were adopted from a previous study (Farhan et al. 2016b) on the basis of compaction requirements in accordance with BS EN 13286-4:2003 through vibrating hammer compaction. For the mixtures stabilized with 3%, 5% and 7% cement, moisture contents of 4.5%, 4.6% and 4.7% (by dry weight of aggregate plus cement mixture) were used, respectively.

3.3 Specimen manufacturing and curing

Variation due to the change of aggregate gradation, which may change the density of the mixture, was eliminated by batching, mixing and compaction each specimen individually. The mixing and other preparatory steps were conducted according to the procedure reported in Farhan et al. (2015). In this procedure, cement was added first to the fine dry aggregate material, then the product was mixed for 60 sec. with other aggregate fraction sizes including rubber aggregate. Then, a mixing for 120 sec. was conducted after adding the design moisture content. Oiled prismatic steel moulds of 100mm x 100mm x 500mm dimensions were used for specimens' fabrication. Once the mixing was finished, a vibrating hammer was utilized to compact the mixture inside the prepared moulds in three layers. Each compacted layer was scarified before compaction the next layer. To ensure accurate characterization, previous investigations (Farhan et al. 2015) suggested manufacturing the specimens with a height slightly greater than required so as to facilitate obtaining a smooth surface by trimming the

excess thickness as shown in Figure 2a and 2b. Three specimens per mix were fabricated and tested and the average value was presented. Once compaction was achieved, specimens were left covered in their moulds to prevent moisture loss. Then, these were demoulded on the next day, wrapped with cling film and stored in wet plastic bags for the curing period (28-days).

4 Testing methodologies and procedures

4.1 Quantification of flexural behaviour under static loading

A 200 kN capacity UTM was used to perform static 4-point flexural testing. Deformation controlled (0.05 mm/min) testing was adopted in this study. For each load application, the deflection at mid span was measured through two LVDTs. The average value of transducers readings was adopted as the deflection for each load application. Figure 2c shows the static flexural testing setup. The following formula was used to compute the flexural strength

$$FS = \frac{F_p \cdot L}{B \cdot H^2} \quad (1)$$

where FS=flexural strength, L= span, F_p =peak force, B=specimen cross-section width and H=specimen cross-section height. Flexural stiffness modulus was calculated based on the elastic part of the load-deformation relationship by adopting 30% of the peak force and the corresponding deflection (Arnold et al. 2012). The following equation was used to calculate stiffness modulus (E_f) value:

$$E_f = \frac{23F \cdot L^3}{108 \cdot B \cdot H^3 \cdot \delta} \quad (2)$$

where δ = mid-span deflection and F= applied force (30% F_u). The water-displacement method was used to estimate the density of specimens after the curing period.

Estimation of flexural toughness was conducted in terms of three parameters which are I_5 , I_{10} and I_{20} , as specified in ASTM C 1018. Toughness index can be estimated as the ratio of area

under the load-deflection curve at specific deflection to the area under the same curve at first crack deflection. These specific deflections are first crack deflection multiplied by 3, 5.5 or 10 when I_5 , I_{10} or I_{20} are being calculated. Ultrasonic Pulse Velocity (UPV) was measured non-destructively via the PUNDIT-plus apparatus in accordance with ASTM C597. In this test, the speed of stress wave between transducer and receiver was measured by the direct transmission method.

4.2 Quantification of flexural behaviour under cyclic loading

Regarding the behaviour under cyclic loading, the same testing configuration as used in static testing was adopted for investigation under cyclic loading. A stress-controlled testing mode at a frequency of 2 Hz. was used (Sobhan and Mashnad 2000). A 25 kN servo-controlled actuator applied the load cyclically at different stress ratios with a haversine waveform (Huang 2004). The repeated load cycles between two values. The maximum one was estimated from the static flexural strength value based on the required stress ratio (SR). About one-tenth of the SR-based load (Sobhan and Mashnad 2000) was applied as a minimum load so as to prevent any impact and hence to ensure accurate response measurement via instruments. Hence, a compression-compression loading was adopted.

Regarding instrumentation and data acquisition, an external high-speed data acquisition device was used since the idea was to identify the behaviour under cyclic flexural loading in terms of damage accumulation during fatigue testing. To this end, the load-mid span dynamic deflection data was acquired at a rate of 20 points per second since this would ensure sufficient data to describe a load-deflection cycle as reported by Sobhan (1997). Figure 3 shows the cyclic loading test setup.

In this paper, the fatigue life was defined by the full collapse point since, in the case of stress-controlled fatigue testing, there is negligible difference between a stiffness reduction criterion and the full collapse point (Li 2013). Flexural dynamic modulus was calculated based only on the recoverable deformation occurred during fatigue testing using the following equation (Sobhan and Mashnad 2003):

$$E_d = \frac{23F_c \cdot L^3}{108 \cdot B \cdot H^3 \cdot \delta_r} \quad (3)$$

where: E_d = flexural dynamic modulus; F_c = applied cyclic force; δ_r = recoverable dynamic deformation. L , B and H are as defined previously.

4.3 Cracking behaviour quantification

A recent investigation conducted by Farhan et al. (2015) indicated that flexural-induced cracks in prismatic samples of different rubber contents propagated through rubber particles. They evidenced this by noting the quantity of crumb rubber particles located on the flexural-fractured surfaces. In this paper, it was intended to validate and ascertain whether mixtures with different amounts of cement will experience the same crack propagation mechanism. To this end, the same previous methodology has been used in this research. In the first place, a high resolution camera was used for capturing the fractured surface images. The captured images were then converted from Red-Green-Blue (RGB) mode to an eight bytes greyscale. This was then filtered and thresholded and finally the quantity of rubber particles was estimated. Figure 4 shows the image processing methodology used in this paper. ImageJ software was used in all the above image processing and calculation steps. Then, the rubber quantity on the fractured surfaces was compared with that used in manufacturing.

5 Results and interpretation

5.1 Behaviour under static flexural loading

5.1.1 Influence of stabilizer quantity on flexural strength and density

Table 3 shows densities of prisms manufactured from different amounts of rubber and cement. As clearly seen from Table 3, the cement content has a slightly positive impact on the density of compacted mixtures due to its filling of the voids between larger particles.

Figure 5 shows that using a greater quantity of cement improved the flexural strength of conventional and rubber-modified mixtures which is obvious since such usage will increase hydration products. This, in turn, enhances the bond strength between aggregate particles and adjacent materials. The same figure also shows that the rubber inclusion at all cementation levels results in a drop in flexural strength value. The difference between the strength of rubber and natural aggregate is the main reason behind this drop in the material's strength. In addition, the high difference between the stiffnesses of rubber aggregate and other surrounding materials will make the rubber particles behave like voids. This, in turn, will increase the stress concentration around the rubber particles since surrounding materials absorb more stresses due to the high stiffness mismatch between these and rubber particles and, accordingly, initiate the cracks at the rubber particles.

5.1.2 Influence of stabilizer quantity on load-deformation relationships and toughness

Load-deformation curves for most of the investigated mixtures are shown in Figure 6. These curves are used for toughness indices estimation as stated earlier in Section 4.1. While there is clear improvement in material toughness due to rubber modification (Figure 7), increasing stabilizer content seems to be of no obvious effect. The indices I_5 , I_{10} , I_{20} for the CBAMs and RCBAMs showed the same behaviour at different cement contents. The likely interpretation is that, when a crack at micro-level reaches a rubber aggregate particle, the latter tends to absorb

and make a relaxation of the stress at the crack tip. Moreover, since the cracks propagate through rubber particles, such operation cause a lengthening of crack path.

5.1.3 Influence of stabilizer quantity on static flexural modulus of elasticity

It is evident from Figure 8 that similar trends for CBAMs and RCBAMs exist where both showed an increase in their static stiffness modulus when the amount of stabilizer was increased in the mixtures with the same rate of improvement. However, it seems that the use of cement content of more than 5% has little effect compared to increasing cement content from 3% to 5%. It is known that the ability of the cemented pavement layer to absorb more stresses is dependent on its stiffness compared to the stiffness of other layers in pavement structure. Consequently, increasing stabilizer quantity in the mixtures beyond 5% does not affect the stress attractiveness of the layer. Rubber inclusion decrease the flexural stiffness of stabilized layer at all examined stabilizer contents as presented in the same figure, which is expected in the light of the very low stiffness of rubber aggregate particles compared to the stiffness of the natural aggregate replaced. This will have a negative impact on stress attraction. And since a cemented layer is normally brittle and sensitive to overloading and fatigue, such stiffness reduction will reduce the attracted stress in the materials (when they are used within the pavement structure) and also results in less fatigue sensitivity under vehicular loading. The latter issue will be discussed in Section 5.2.

5.1.4 Influence of stabilizer quantity on Ultrasonic Pulse Velocity (UPV)

The value of ultrasonic pulse velocity increases (Figure 9) as the amount of cement increase in the stabilized mixtures in a similar trend as observed in the case of static modulus of elasticity. This can be explained in the light of the amount of voids in the mixture which greatly affects the wave transmission speed. To some extent, using a higher amount of cement reduces the voids due to its filling effect. As is well understood, the hydration products increases as the amount of cement increase. For this reason, Bogas et al. (2013) justified the low voids in the

mixtures of higher cement content. Mohammad (2011) and Su et al. (2013) observed similar behaviour.

As can be seen from Figure 9, UPV decreased with rubber incorporation at all investigated cement contents. The low stiffness modulus of the rubber aggregate seems to be the main reason behind the reduction of the UPV value as reported by Zheng et al. (2008). Aggregate interlocking reduction in the case of rubber inclusion might be another contributory reason behind the drop of UPV. This interlocking reduction would reduce the contact points between natural aggregate of high stiffness which, in turn, reduces the transmission efficiency of ultrasonic wave. Moreover, the high elasticity nature of rubber aggregate causes them to absorb some of the wave energy. As for elastic modulus behaviour (Figure 8), the improvement of wave velocity seems more obvious for stabilized mixture in which the amount of stabilizer increased from 3% to 5% while little improvement occurs beyond that amount of stabilization.

5.2 Behaviour under cyclic flexural loading

5.2.1 Influence of stabilizer quantity and rubber on the fatigue of CBAMs

The fatigue life seems to be increased as a result of rubber inclusion for all investigated mixtures containing various amounts of cement as shown in Figure 10. Such increase is more obvious at 7% cement content and seems to be a stress-dependent phenomenon where, at a stress ratio of 90%, no clear behaviour exists while mixtures of different cement contents have longer fatigue life after rubber modification. The reason behind this might be due to the period of the microcracking phase. The latter stage is normally longer in the case of stress-controlled mode at lower stress ratio. In one study, Farhan et al. (2016a) proved that cracks initiated and propagated through rubber particles and that such a mechanism is responsible for toughness improvement. They reported that at a microcracking level, rubber particles tend to relieve the

stresses generated at the crack tip. Such a process retards the propagation of cracks which in turn enhances material toughness. The later improvement seems to be directly related to the behaviour of the rubberized mixtures when they are subjected to repeated loading. This findings are consistent with the conclusion reported by Modarres and Hosseini (2014). This is also consistent with the outcomes of the toughness explanation mentioned above. From these findings and that stated earlier in in Section 5.1.2 (Figure 7), it can be concluded that there is a proportional relationship between toughness and the fatigue life. Moreover, the suggested mechanism of toughness improvement is behind the improvement of the fatigue life.

5.3 Evaluation of damage accumulation

Total deflection (recoverable plus permanent) were recorded for each cycle. A sample of such total deflections is illustrated in Figure 11. For each cycle, the maximum (red line) and minimum (green line) deflection were extracted during the fatigue life. It is necessary, for the purpose of monitoring the stiffness modulus along the fatigue life, to calculate the recoverable deflection for each cycle. The latter parameter was calculated from the difference between the maximum and minimum deflections. It can be clearly seen from the deflection profiles presented in Figure 11 that, in the case of stress ratio of 90%, there are two regions. The first extends from the beginning until almost 95% and 90% of the fatigue life for 3% and 7% cement contents, respectively. On the other hand, three regions appear when a stress ratio of 85% is applied regardless of rubber or cement content.

5.3.1 Permanent deformation accumulation

Permanent deformation accumulates gradually, during fatigue, and is an indication that the damage accumulated in the specimen as reported by Grzybowski and Meyer (1993). Figure 12 illustrates the influence of cement quantity on the plastic deformation accumulation for CBAMs

and RCBAMs. With exception of mixtures containing 3% cement content which showed a slightly higher permanent deformation, all other investigated mixtures presented low degree of permanent deformation. Once again, this can be attributed to the microcracking phase duration that occurs at high stress ratios. The microcracking phase is very short at this stress condition especially at 5% and 7% cement contents. It was followed by the macrocracking phase which resulted in the collapse of the specimen without excessive deflection. However, at low stress ratio (85%), specimens containing crumb rubber with various cement contents experienced a higher level of permanent deformation. The highest permanent deformation occurred when 7% cement content was used. The above explanation supports the interpretation of the fatigue life improvement mentioned above in Subsection 5.2.1.

The rate of microcracking development in concrete specimens under cyclic load was observed non-destructively by Shah and Chandra (1970). Their results indicated that the microcracking development was stable and slow in the case of 70% and below stress ratio whereas at 80% and higher, the rate of microcrack growth was faster. Such a conclusion is consistent with the current findings.

Permanent deformation is also a stress ratio-dependent parameter as illustrated in Figure 12. Comparing Figure 12 (a and b) with Figure 12 (c and d) indicates that the rate of permanent deformation at 90% stress ratio was not affected by rubber modification of the mixtures regardless of cement content. In contrast, at low stress ratios, a greater damage accumulation occurred after rubber inclusion. Mixtures containing 7% cement content experienced larger degrees of damage accumulation. In addition, rubber incorporation resulted in greater deformation at failure.

The above finding indicates that the fatigue life of the material is related to the rate of damage accumulation where mixtures experiencing higher damage accumulation last longer under

cyclic loading. This finding indicates and confirms that the inclusion of rubber particles reduces the sensitivity to the fatigue cracking by accommodating more accumulated damage. Sobhan and Mashnad (2002) studied the behaviour of roller-compacted concrete under fatigue loading. Their results revealed similar permanent deformation growth.

5.3.2 Degradation of dynamic modulus

Modulus of elasticity is one of the required inputs for pavement analysis and design. In the latter process, this parameter is assumed to be constant along with the fatigue life of the pavement layer. Since the dynamic modulus degrades with time as a result of internal damage of the materials, the idea of constant modulus seems inaccurate as reported by (Oliveira 2006). Such inaccuracy increase for materials of higher degradability since the stiffness modulus change significantly during the service life of the pavement layer. Consequently, it is important to ascertain that the materials do not have higher degree of degradation. Furthermore, such observation may also help understanding of behaviour and damage processes of both types of mixtures under repeated loading. So, in this part of study, the degradation of stiffness modulus is also quantified under such loading to best reveal the role of rubber particles in that degradation process.

Comparison of Figure 13 (a and b) with Figure 13 (c and d) reveals that there is no clear impact of the rubber particles inclusion on the degradability of the stiffness modulus. For mixtures stabilized with 3% cement content, a larger degree of degradability was observed. A greater dynamic modulus degradation would necessitate increasing layer thickness to ensure the same stress/strain level in the layers above and below the layer made of this degradable material. Therefore, layers stabilized with low cement content would require increase their thickness to allow for the dynamic modulus degradation in the structural design. However, rubber particles

have no effect on the stiffness degradability and the rubberized mixtures do not differ from reference mixtures.

For the majority of tested specimens, dynamic modulus degradation profiles showed two regions. The first one was between 0 and 95% of the fatigue life. Then, this was followed by a rapid degradation stage. In his study, Paul (2011) examined the degradation of lightly stabilized materials and presented similar behaviour which is consistent with the outcomes of the current study.

5.4 Cracking patterns and behaviour

Figure 14 shows the patterns of cracking of specimens made of stabilized mixtures containing different amounts of stabilizer. As this figure indicates, the predominate failure pattern in the case of low stabilization status is the propagation of cracks around aggregate particles (i.e., aggregate dislocation due to low bond strength). In mixtures stabilized with 5% cement content, there are two failure modes which are aggregate fracturing and aggregate dislocation. Finally, the highly cemented specimens experienced, almost aggregate fracturing.

This can be attributed to the bond strength between aggregates and the surrounding matrix which is governed by different cement contents that also controls the density of the adjacent matrix (fine and cement) and formation of hydration products that gives a reasonable bond strength. Another contributory factor is the extent of water-cement slurry penetration into aggregate particles under vibrating hammer compaction.

As can be seen from Figure 15, for all cement contents, the amount of rubber observed on the fractured surface was greater than that originally used in the preparation of the rubberized sample. This indicates that the propagation of cracks preferentially occurred through the rubber

aggregate. However, at low cement content (3%), the difference between the two rubber quantities was small as compared with that at 5% and 7%. This indicates a reduced tendency for cracks to propagate through the rubber particles. It seems that the reason behind this phenomenon is that, at 5% and 7%, the rubber particles were much the weakest points in the cemented samples, attracting the cracks while, in weakly cemented mixtures, the weak bond between aggregate particles and surrounding matrix represented alternative and almost equally weak points.

In another investigation, Farhan et al. (2016) utilized X-ray CT scans of samples that had failed under indirect tensile loading and confirmed that the crack propagation was through the rubber particles. This explanation supports the hypothesis given above regarding the mechanism behind the toughness improvement due to rubber incorporation (Section 5.3).

6 Conclusions

In this paper, a laboratory investigation was undertaken to study the role of stabilizer quantity on both the static and dynamic behaviour of conventional and rubber-modified cemented granular mixtures. The main conclusions revealed from this study can be listed as follows:

1. Flexural strength improved for conventional and rubberized cemented mixtures containing higher amounts of stabilizer while replacing natural aggregate with rubber aggregate declines the flexural strength for all investigated mixtures regardless of different stabilizer contents. Toughness improvement occurred due to rubber modification at all stabilization levels but increasing cement content has no clear impact on toughness of both the conventional and rubberized mixtures.
2. Crumb rubber inclusion reduced the flexural stiffness modulus at all stabilization levels. The greater drop occurred in mixtures containing 3% cement content. This behaviour was

further observed utilizing non-destructive testing and is consistent with that observed under indirect tensile loading reported in previous research.

3. Examination of the flexural-induced fractured surfaces revealed that the propagation of cracks occurred through or adjacent to the rubber aggregate at different levels of stabilization. This reinforces previous findings and also provides a reason for the flexural toughness improvement.

4. Fatigue life improved after rubber inclusion at different stabilizer contents since rubber particles tends to absorb stress at the microcrack tip. The benefits of rubber particles over the fatigue life appeared most significantly at lower stress ratios since the latter ensured a reasonable microcracking period.

5. Moderate and high stabilization degrees ensure less degradable mixtures while lightly cemented mixtures showed higher degradability. Despite their higher elasticity, rubber particles have no noticeable effect on the dynamic modulus degradation of cemented aggregate mixes which in turn ensures they do not affect adversely the stress level in the stabilized layer over the design life.

6. It seems that the rubber resists and relieves the stresses at crack tips when they are at the microcracking stage, and for this reason, the effectiveness of the rubber appeared at lower stress ratio are not at a higher stress ratio. Thus, embedding rubber particles in a cement-stabilized layer of enough thickness, to ensure a low stress ratio, may be useful in relieving the stresses inside this layer and improving the life under cyclic loading.

Acknowledgements

The support from the Higher Committee of Education Development in Iraq (HCED) is gratefully acknowledged. Authors also would like to express their thanks to Mr. Balbir Loyla, the Senior Technician at the Small Structures Laboratory, University of Nottingham, for helping to conduct static and cyclic testing.

Table 1: Properties of limestone aggregate.

Property	Aggregate fraction size (mm)				
	20	14	10	6	Dust
Oven dried density, Mg/m ³	2.633	2.607	2.608	2.427	2.668
Saturated surface dried density, Mg/m ³	2.653	2.634	2.640	2.526	2.674
Apparent, Mg/m ³	2.685	2.679	2.693	2.696	2.686
Water absorption, %	0.74	1.03	1.2	4.1	0.26

Table 2: Physical and chemical properties of cement.

Property	Determined as
Specific gravity	3.15
Fineness	420
Oxide	Determined as (%)
SiO ₂	19.6
Al ₂ O ₃	4.9
Fe ₂ O ₃	3.1
CaO	63.1
MgO	1.2
SO ₃	3.4
LOI	2.7
Chloride as Cl	0.05
Alkalis as (Na ₂ O)	0.74

Table 3: Densities of reference and rubberized mixtures

Mixture	Stabilizer content, %		
	3	5	7
CBAMs	2512.90	2529.65	2526.03
Std. Deviation	24.37	2.59	3.49
CoV	0.0097	0.00103	0.00138
RCBAMs	2449.30	2456.43	2462.50
Std. Deviation	3.46	4.94	3.50
CoV	0.00141	0.00201	0.00142

Figure captions

Figure 1: Design gradation for aggregate mixture.

Figure 2: Some preparatory steps: a. specimen trimming; b. appearance of trimmed specimen and c. static flexural testing arrangement.

Figure 3: Cyclic flexural testing setup.

Figure 4: Estimating the amount of rubber in the fractured surface.

Figure 5: Flexural strength for both conventional and rubber-modified mixtures.

Figure 6: Load-deflection curves for combination of rubber and cement quantity: a. C3R0; b.C3R30; c. C7R0 and d.C7R30.

Figure 7: Toughness indices for conventional and rubber-modified mixtures.

Figure 8: Static flexural stiffness for conventional and rubber-modified mixtures.

Figure 9: UPVs for conventional and rubber-modified mixtures.

Figure 10: Influence of cement quantity on fatigue lives of CBAMs and RCBAMs at stress ratio of 90% and 85%.

Figure 11: Typical deflection-normalized cycles relationships for some investigated mixtures at 90% stress ratio: a. C3R0, b.C3R30, c. C7R0 and d. C7R30.

Figure 12: Permanent deformation accumulation across fatigue life for some investigated mixtures at 90% and 85% stress ratio: a. C3R0, b.C3R30, c. C7R0 and d. C7R30.

Figure 13: Dynamic modulus degradation across fatigue life: a. rubberized mixtures at stress ratio 85%, b. rubberized mixtures at stress ratio 90%, c. references mixtures at stress ratio 85% and d. references mixtures at stress 90%.

Figure 14: Fractured surfaces: a. C3R0, b.C3R30, c. C5R0 and d. C5R30, e. C7R0 and f. C7R30. Black and red arrows indicate to failure around aggregate and through aggregate, respectively.

Figure 15: Amount of rubber in the fractured surfaces for conventional and rubber-modified mixtures.

Figure 1: Design gradation for aggregate mixture.

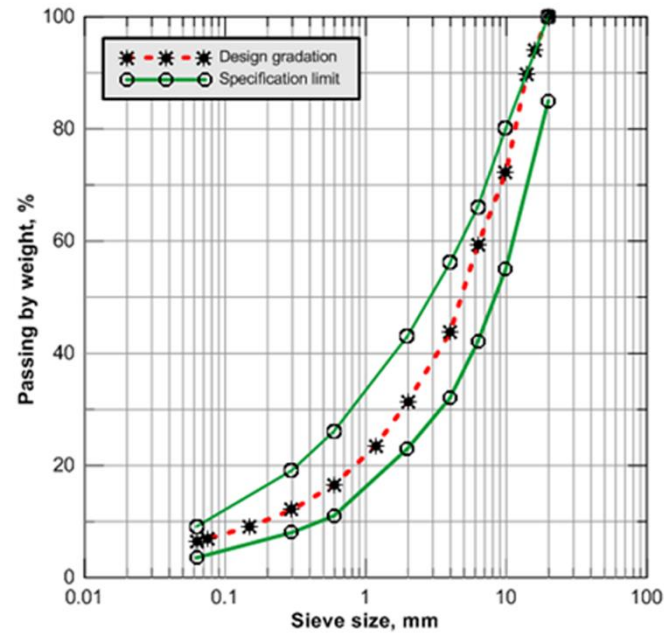


Figure 2: Some preparatory steps: a. specimen trimming; b. appearance of trimmed specimen and c. static flexural testing arrangement.



Note: Blocks with small gap above are placed to prevent the large deflection post-failure, so as to stop instrument damage

Figure 3: Cyclic flexural testing setup.

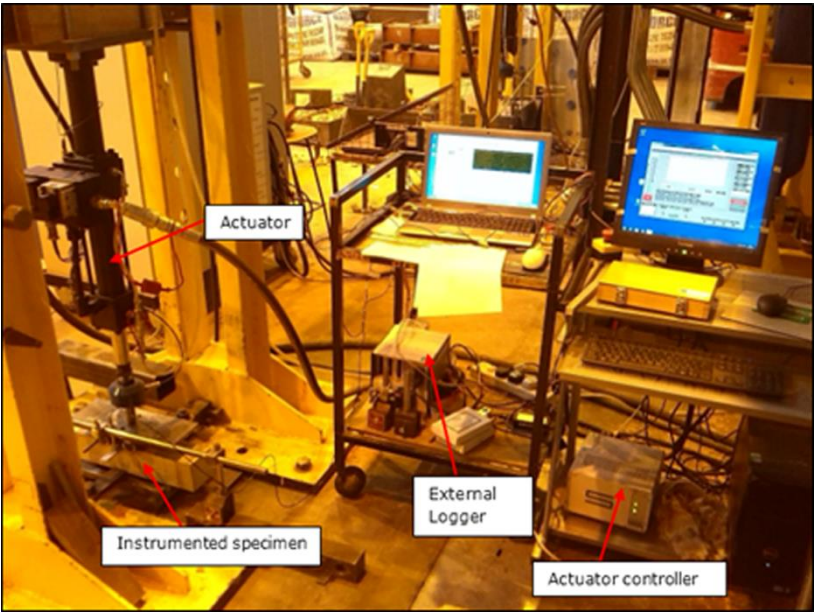


Figure 4: Estimating the amount of rubber in the fractured surface.

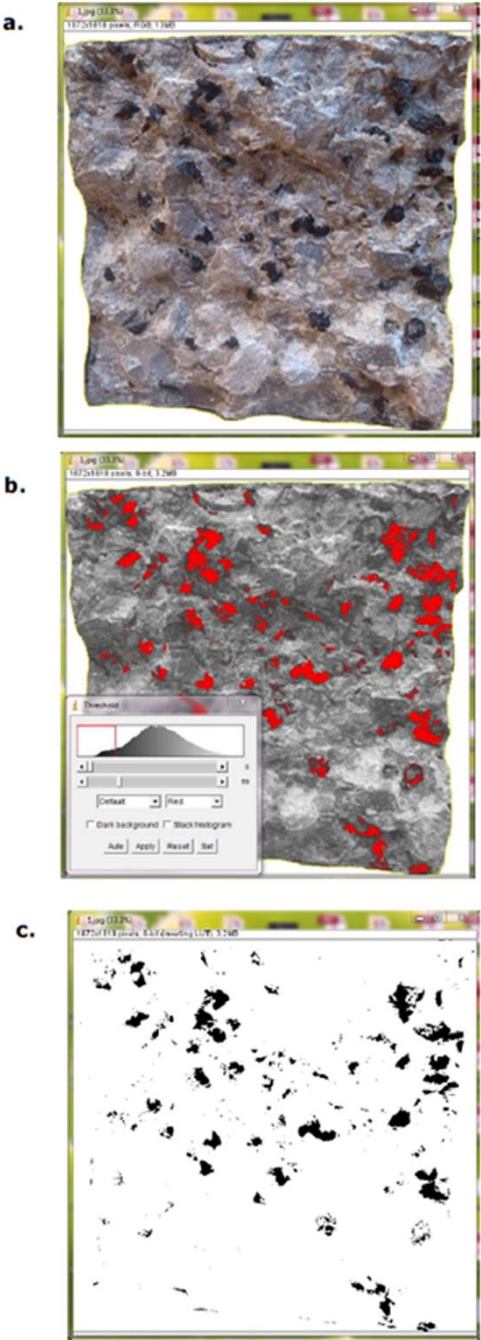


Figure 5: Flexural strength for both conventional and rubber-modified mixtures.

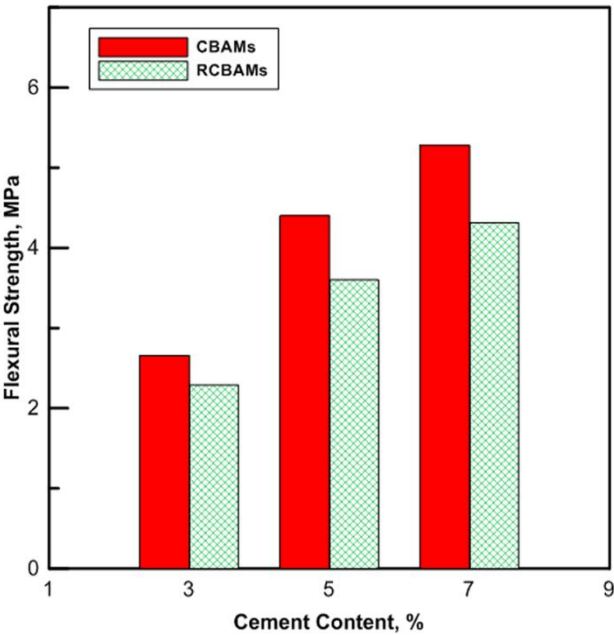


Figure 6: Load-deflection curves for combination of rubber and cement quantity: a. C3R0; b.C3R30; c. C7R0 and d.C7R30.

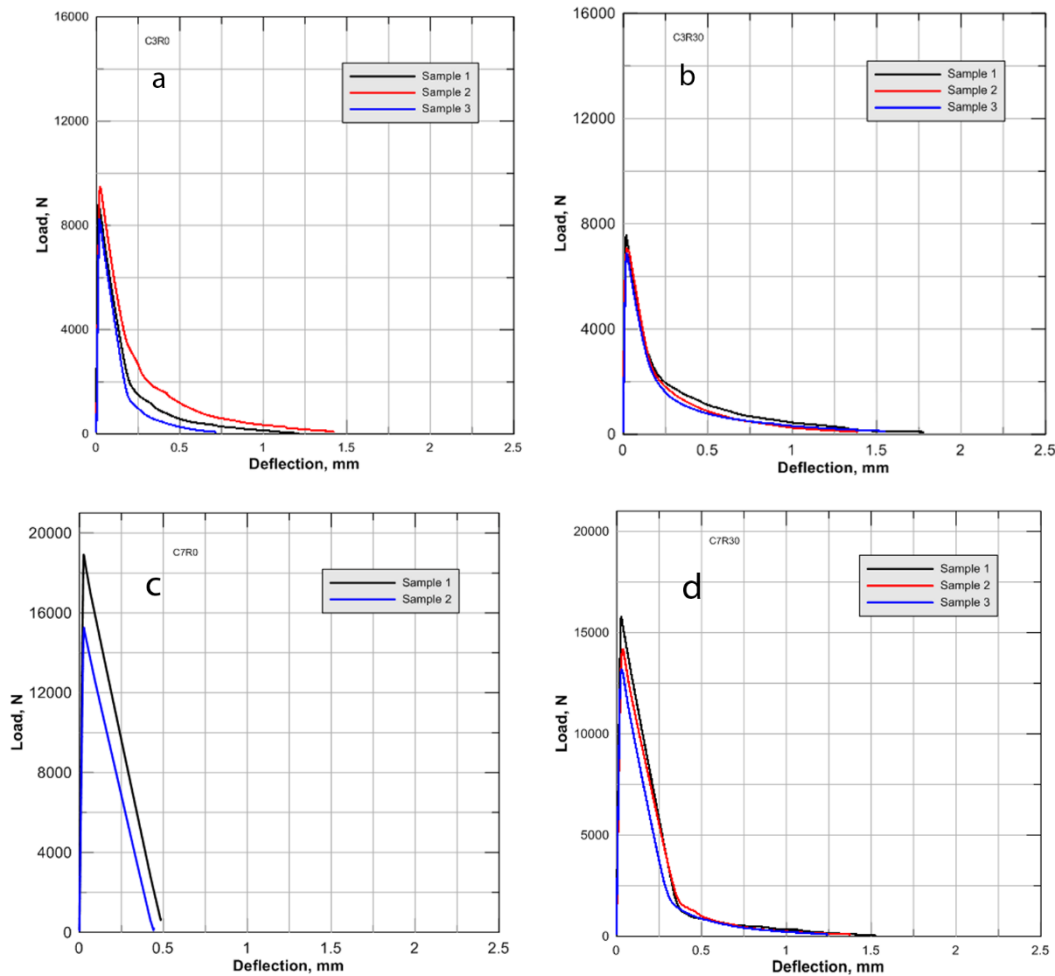


Figure 7: Toughness indices for conventional and rubber-modified mixtures.

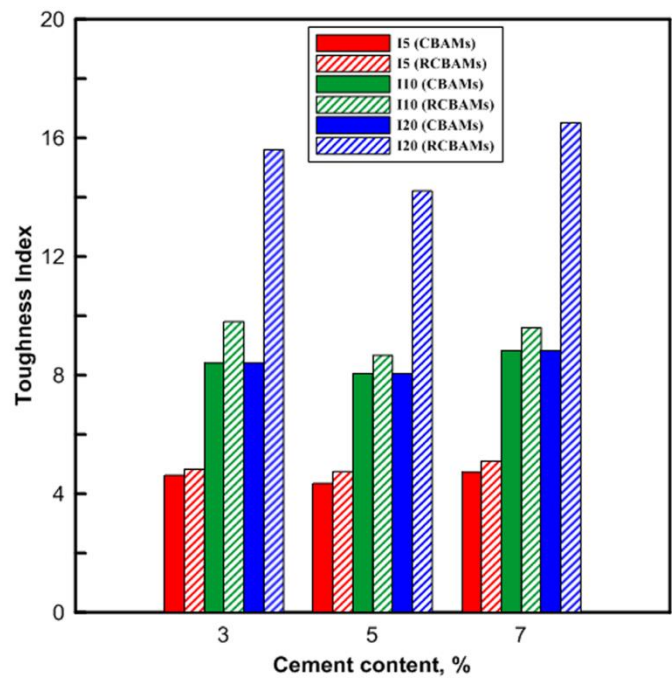


Figure 8: Static flexural stiffness for conventional and rubber-modified mixtures.

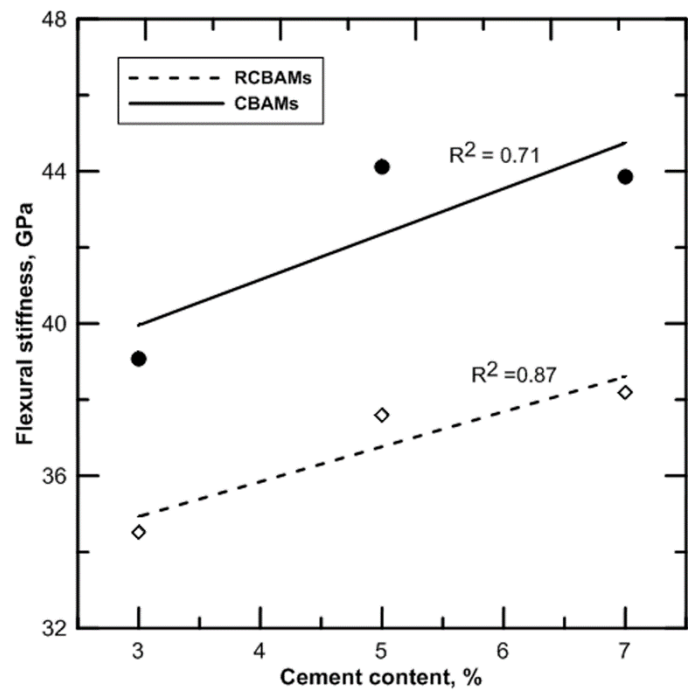


Figure 9: UPVs for conventional and rubber-modified mixtures.

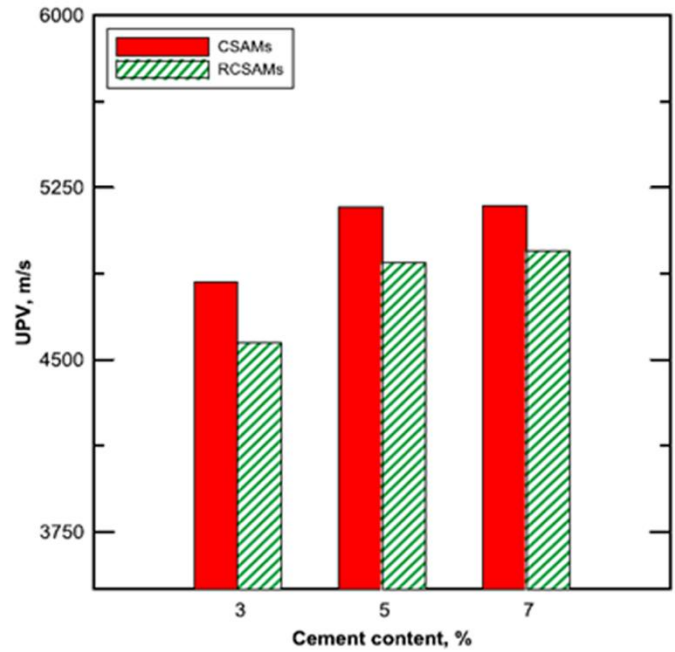


Figure 10: Influence of cement quantity on fatigue lives of CBAMs and RCBAMs at stress ratio of 90% and 85%.

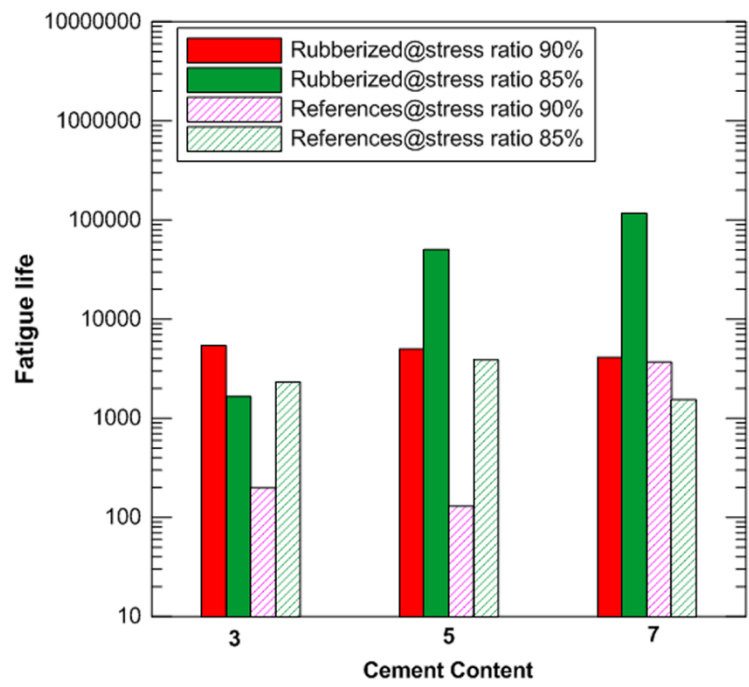


Figure 11: Typical deflection-normalized cycles relationships for some investigated mixtures at 90% stress ratio: a. C3R0, b.C3R30, c. C7R0 and d. C7R30.

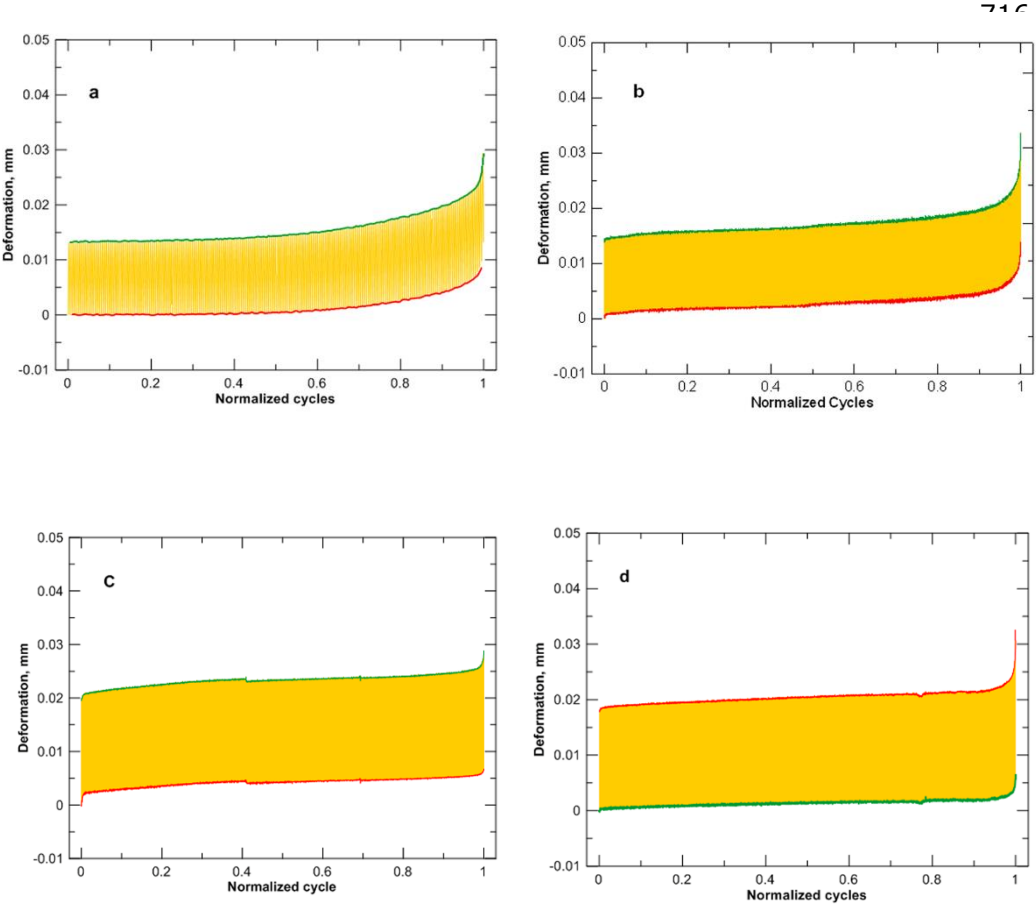


Figure 12: Permanent deformation accumulation across fatigue life for some investigated mixtures at 90% and 85% stress ratio: a. C3R0, b.C3R30, c. C7R0 and d. C7R30.

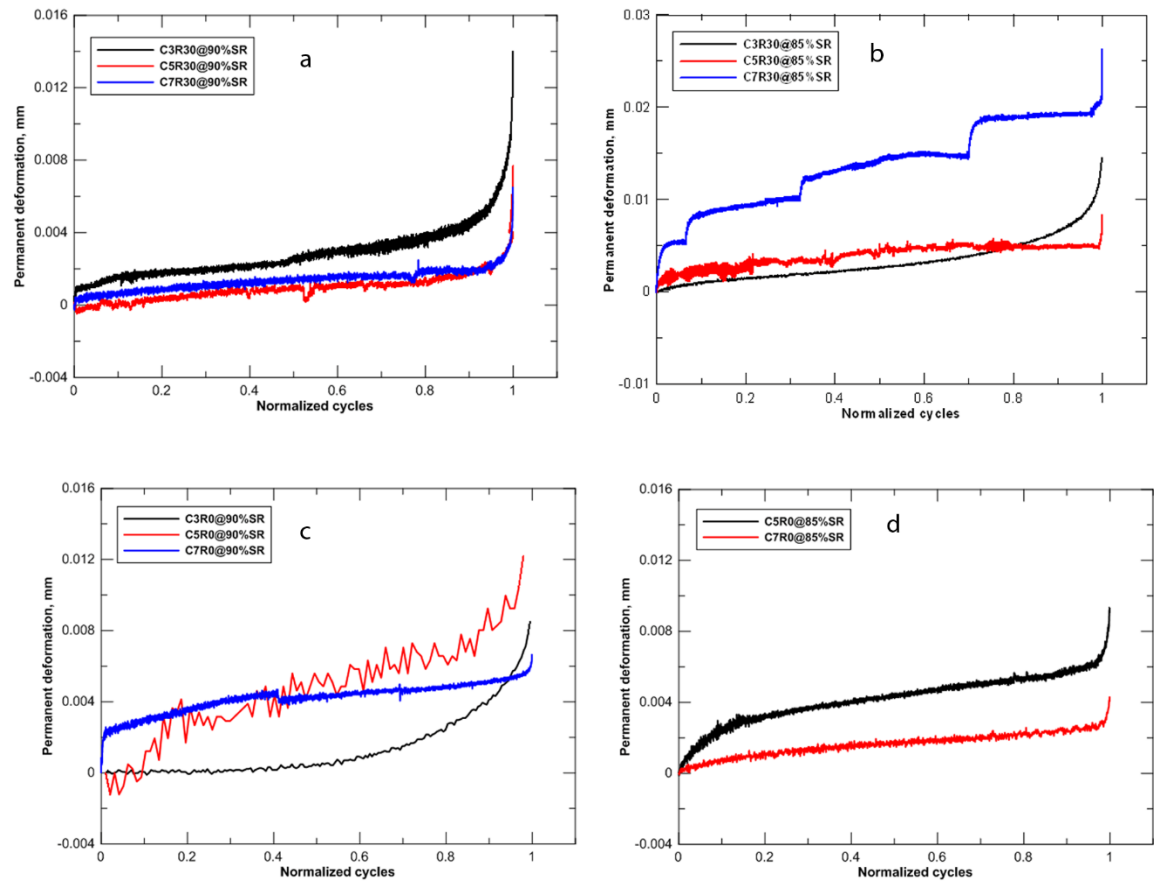


Figure 13: Dynamic modulus degradation across fatigue life: a. rubberized mixtures at stress ratio 85%, b. rubberized mixtures at stress ratio 90%, c. references mixtures at stress ratio 85% and d. references mixtures at stress 90%.

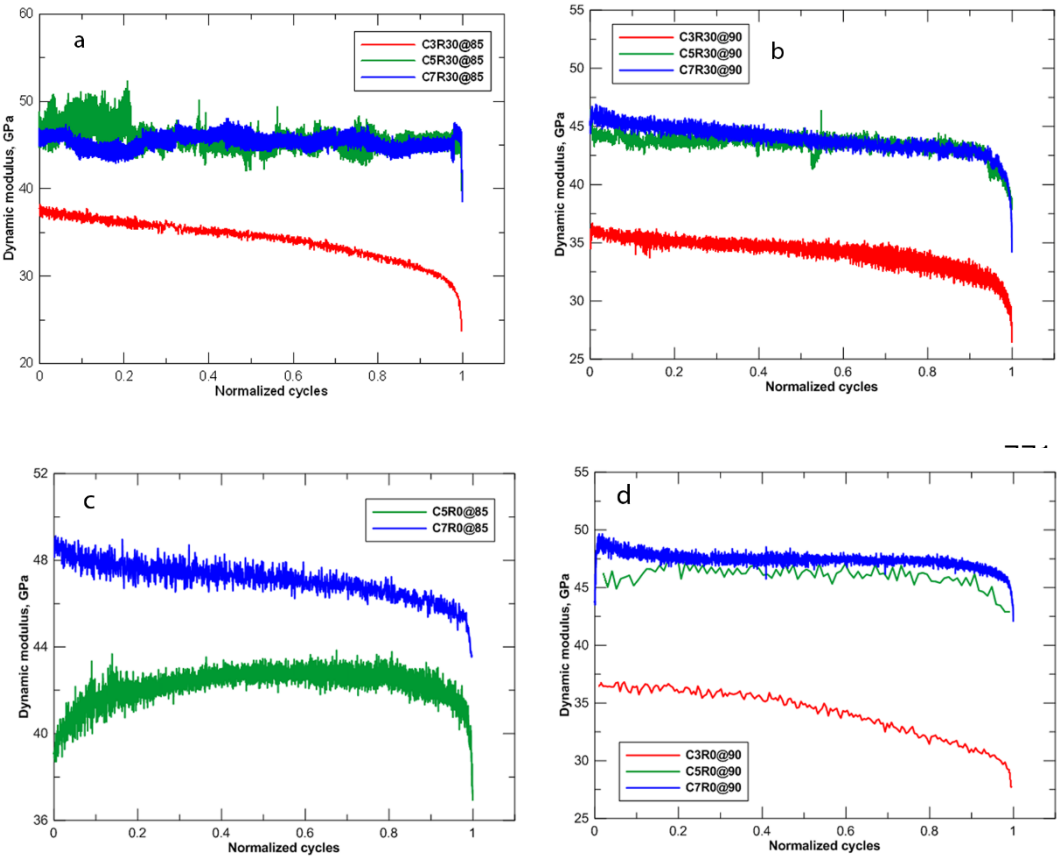


Figure 14: Fractured surfaces: a. C3R0, b.C3R30, c. C5R0 and d. C5R30, e. C7R0 and f. C7R30. Black and red arrows indicate to failure around aggregate and through aggregate, respectively.

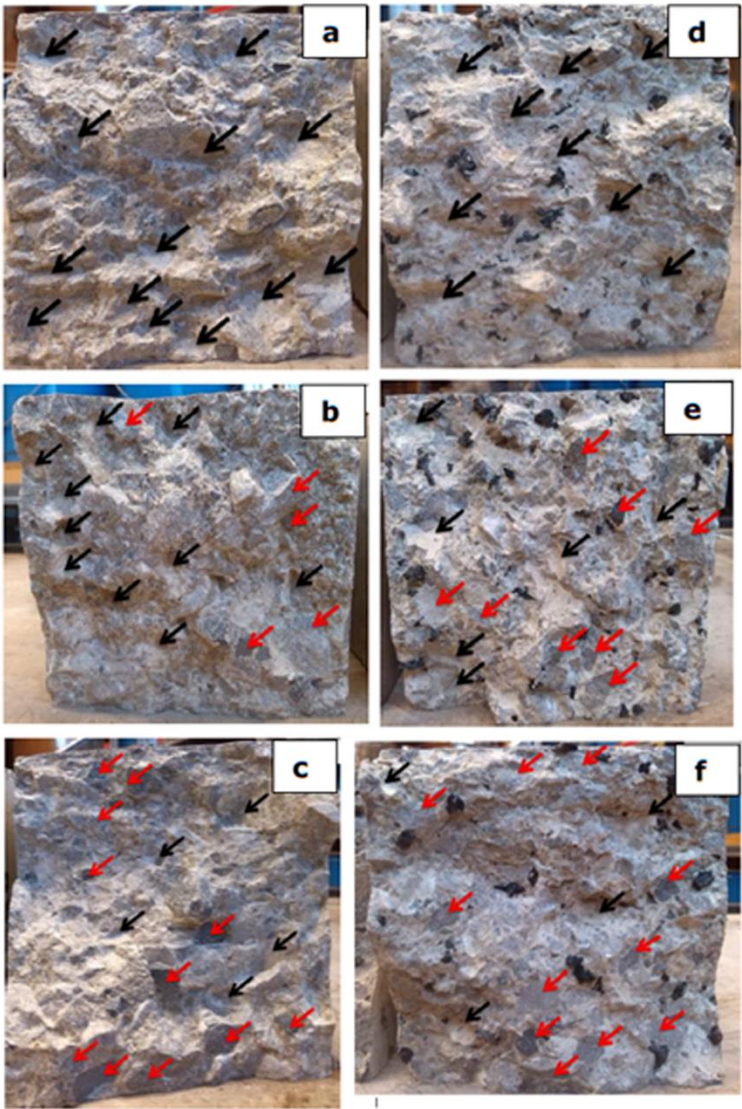
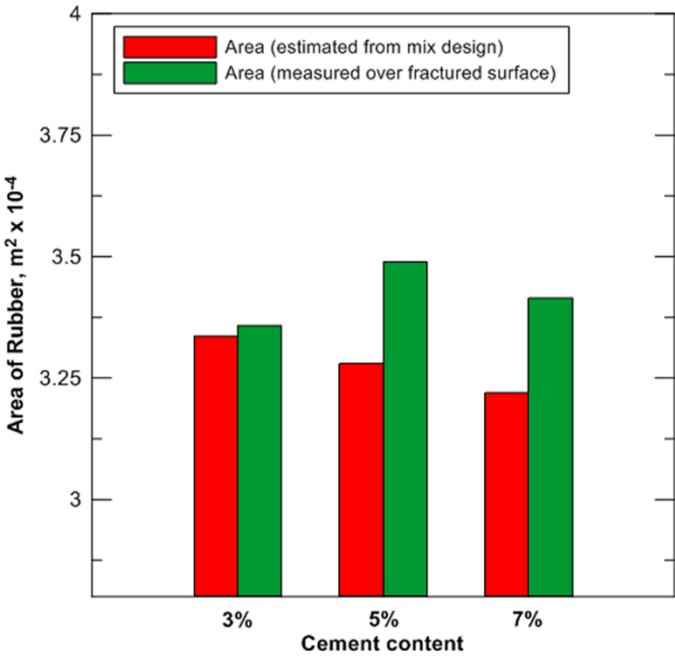


Figure 15: Amount of rubber in the fractured surfaces for conventional and rubber-modified mixtures.



853 **References**

- 854 Arnold, G., Morkel C. and van der Weshuizen G. (2012). Development of tensile fatigue
855 criteria for bound materials, NZ Transport Agency report No. 463, New Zealand Institute
856 of Highway Technology.
- 857 Arulrajah, A., Disfani M. M., Haghighi H., Mohammadinia A. and Horpibulsuk S. (2015).
858 "Modulus of rupture evaluation of cement stabilized recycled glass/recycled concrete
859 aggregate blends." Construction and Building Materials **84**: 146-155.
- 860 Barišić, I., Dimter S. and Rukavina T. (2014). "Strength properties of steel slag stabilized
861 mixes." Composites Part B: Engineering **58**: 386-391.
- 862 Bogas, J. A., Gomes M. G. and Gomes A. (2013). "Compressive strength evaluation of
863 structural lightweight concrete by non-destructive ultrasonic pulse velocity method."
864 Ultrasonics **53**(5): 962-972.
- 865 Cao, W. (2007). "Study on properties of recycled tire rubber modified asphalt mixtures
866 using dry process." Construction and Building Materials **21**(5): 1011-1015.
- 867 Eiras, J., Segovia F., Borrachero M., Monzó J., Bonilla M. and Payá J. (2014). "Physical and
868 mechanical properties of foamed Portland cement composite containing crumb rubber from
869 worn tires." Materials & Design **59**: 550-557.
- 870 Farhan, A. H., Dawson A. R. and Thom N. H. (2016a). "Characterization of rubberized
871 cement bound aggregate mixtures using indirect tensile testing and fractal analysis."
872 Construction and Building Materials **105**: 94-102.
- 873 Farhan, A. H., Dawson A. R. and Thom N. H. (2016b). "Effect of cementation level on
874 performance of rubberized cement-stabilized aggregate mixtures." Materials & Design **97**:
875 98-107.
- 876 Farhan, A. H., Dawson A. R., Thom N. H., Adam S. and Smith M. J. (2015). "Flexural
877 characteristics of rubberized cement-stabilized crushed aggregate for pavement structure."
878 Materials & Design **88**: 897-905.
- 879 Garber, N. J. and Hoel L. A. (2009). Traffic & highway engineering, Cengage Learning.
- 880 Grzybowski, M. and Meyer C. (1993). "Damage accumulation in concrete with and without
881 fiber reinforcement." ACI Materials Journal **90**(6).
- 882 Güneyisi, E., Gesoğlu M. and Özturan T. (2004). "Properties of rubberized concretes
883 containing silica fume." Cement and Concrete Research **34**(12): 2309-2317.
- 884 Huang, Y. H. (2004). Pavement analysis and design, Second edition, Prentice Hall
885 Publishing company, 792 pages.
- 886 Khaloo, A. R., Dehestani M. and Rahmatabadi P. (2008). "Mechanical properties of concrete
887 containing a high volume of tire-rubber particles." Waste Management **28**(12): 2472-2482.
- 888 Li, N. (2013). Asphalt Mixture Fatigue Testing: Influence of Test Type and Specimen Size.
889 PhD Thesis, TU Delft, Delft University of Technology.
- 890 Li, Y., Sun X. and Yin J. (2010). Mix design of cement-stabilized recycled aggregate base
891 course material. Paving Materials and Pavement Analysis: 184-192.
- 892 Modarres, A. and Hosseini Z. (2014). "Mechanical properties of roller compacted concrete
893 containing rice husk ash with original and recycled asphalt pavement material." Materials
894 & Design **64**: 227-236.
- 895 Mohammad, I. K. (2011). Non-Destructive Testing for Concrete: Dynamic Modulus and
896 Ultrasonic Velocity Measurements. Advanced Materials Research, Trans Tech Publ.
- 897 Oikonomou, N. and Mavridou S. (2009). "The use of waste tyre rubber in civil engineering
898 works." Sustainability of construction materials. WoodHead Publishing Limited, Abington
899 Hall, Cambridge.
- 900 Oliveira, J. R. M. d. (2006). Grouted macadam: material characterisation for pavement
901 design. PhD Thesis, University of Nottingham.
- 902 Paul, D. K. (2011). "Characterisation of Lightly Stabilised Granular Materials by Various
903 Laboratory Testing Methods." PhD Thesis, University of New South Wales, Australian.
- 904 Pelisser, F., Zavarise N., Longo T. A. and Bernardin A. M. (2011). "Concrete made with
905 recycled tire rubber: Effect of alkaline activation and silica fume addition." Journal of
906 Cleaner Production **19**(6-7): 757-763.
- 907 Puppala, A. J., Pedarla A., Chittoori B., Ganne V. K. and Nazarian S. (2017). "Long-Term
908 Durability Studies on Chemically Treated Reclaimed Asphalt Pavement Material as a Base
909 Layer for Pavements." Transportation Research Record: Journal of the Transportation
910 Research Board(2657): 1-9.

911 Shah, S. P. and Chandra S. (1970). Fracture of concrete subjected to cyclic and sustained
912 loading. ACI Journal Proceedings, ACI.

913 Sobhan, K. (1997). "Stabilized fiber reinforced pavement base course with recycled
914 aggregates." PhD Thesis, Northwest University, Evanstone, Illinois.

915 Sobhan, K. and Mashnad M. (2000). "Fatigue durability of stabilized recycled aggregate
916 base course containing fly ash and waste-plastic strip reinforcement." Final Rep. Submitted
917 to the Recycled Materials Resource Centre, Univ. of New Hampshire.

918 Sobhan, K. and Mashnad M. (2002). "Fatigue damage in roller-compacted pavement
919 foundation with recycled aggregate and waste plastic strips." Transportation Research
920 Record: Journal of the Transportation Research Board(1798): 8-16.

921 Sobhan, K. and Mashnad M. (2003). "Fatigue behavior of a pavement foundation with
922 recycled aggregate and waste HDPE strips." Journal of geotechnical and geoenvironmental
923 engineering **129**(7): 630-638.

924 Su, Z., Fratta D., Tinjum J. M. and Edil T. B. (2013). Cementitiously Stabilized Materials
925 Using Ultrasonic Testing. Transportation Research Board 92nd Annual Meeting.

926 Thompson, I. (2001). "Use of Steel Fibers to Reinforce Cement Bound Roadbase." PhD
927 Thesis, University of Nottingham.

928 Topcu, I. B. and Avcular N. (1997). "COLLISION BEHAVIOURS OF RUBBERIZED
929 CONCRETE." Cement and Concrete Research **27**(12): 1893-1898,.

930 Xuan, D., Houben L., Molenaar A. and Shui Z. (2012). "Mixture optimization of cement
931 treated demolition waste with recycled masonry and concrete." Materials and structures
932 **45**(1-2): 143-151.

933 Youssf, O., Mills J. E. and Hassanli R. (2016). "Assessment of the mechanical performance
934 of crumb rubber concrete." Construction and Building Materials **125**: 175-183.

935 Zheng, L., Sharon Huo X. and Yuan Y. (2008). "Strength, Modulus of Elasticity, and
936 Brittleness Index of Rubberized Concrete." Journal of Civil Engineering , ASCE.

937